

**Electrospun Poly(N-isopropylacrylamide) / Ethyl Cellulose  
Nanofibers as Thermoresponsive Drug Delivery Systems**

Juan Hu<sup>1</sup>, Heyu Li<sup>1</sup>, Gareth R. Williams<sup>2\*</sup>, Huihui Yang<sup>1</sup>, Tao Lei<sup>1</sup>,

Li-Min Zhu<sup>1\*</sup>

1. College of Chemistry, Chemical Engineering and Biotechnology,  
Donghua University, Shanghai, 201620, China
2. UCL School of Pharmacy, University College London, 29-39  
Brunswick Square, London, WC1N 1AX, UK

\* Authors for correspondence. Email: [g.williams@ucl.ac.uk](mailto:g.williams@ucl.ac.uk) (GRW);  
[lzhu@dhu.edu.cn](mailto:lzhu@dhu.edu.cn) (LMZ). Tel: +44 (0) 207 753 5868 (GRW); +86 21  
6779 2655 (LMZ).

## **Abstract**

Fibers of poly(N-isopropylacrylamide) (PNIPAAm), ethylcellulose (EC) and a blend of both were successfully fabricated by electrospinning. Analogous drug-loaded fibers were prepared loaded with ketoprofen (KET). Scanning and transmission electron microscopy showed that the fibers were largely smooth and cylindrical, with no phase separation observed. The addition of KET to the spinning solutions did not affect the morphology of the resultant fibers, and no drug particles could be observed to separate from the polymer matrix. X-ray diffraction demonstrated that the drug was present in the amorphous physical form in the fiber matrix. There are significant intermolecular interactions between KET and polymers, as evidenced by IR spectroscopy and molecular modelling. Water contact angle measurements proved that the PNIPAAm and PNIPAAm/EC fibers switched from being hydrophilic to hydrophobic when the temperature was increased through the lower critical solution temperature of 32 °C. *In vitro* drug release studies found that the PNIPAAm/EC blend nanofibers were able to synergistically combine the properties of the two polymers, giving temperature-sensitive systems with sustained release properties. In addition, they were established to be non-toxic and suitable for cell growth. This study thus demonstrates that electrospun blend PNIPAAm/EC fibers comprise effective and biocompatible materials for drug delivery systems and tissue engineering.

**Keywords:** poly(N-isopropylacrylamide), ethylcellulose, electrospinning, controlled release, temperature-sensitive, biocompatible materials, contact angle, molecular modelling, morphology, amorphous

## 1. Introduction

Electrospinning comprises a straightforward and cost-effective technique for the fabrication of fibers with dimensions on the nanometer to micron scale.<sup>1,2</sup> Electrospun nanofibers have attracted considerable attention due to their high surface area to volume ratio, narrow diameters, high porosity and often desirable mechanical properties.<sup>3-8</sup> They are attractive for a number of practical applications, such as wound dressing, drug delivery, tissue engineering, medical prostheses, textiles, filtration systems, and sensors, *inter alia*.<sup>9-13</sup>

Responsive polymers exhibit a change in configuration, dimensions, or physicochemical properties following exposure to an external stimulus. This could comprise changes in pH, temperature, electromagnetic field, light or solvent.<sup>14-16</sup> Poly(N-isopropylacrylamide) (PNIPAAm) is one such polymer, and undergoes a sharp phase transition (from linear to globular) at a lower critical solution temperature (LCST) of *ca.* 32 °C in aqueous solution.<sup>17-19</sup> It has been intensively studied for potential applications in biomedicine.<sup>20-22</sup> When the temperature is raised from below to above the LCST, PNIPAAm rapidly changes from being hydrophilic to hydrophobic.<sup>23,24</sup>

While attractive for its thermoresponsive properties, PNIPAAm cannot easily be electrospun. Thus, researchers have resorted to the use of copolymers or blends of PNIPAAm with other polymers to aid the spinning process and enhance the quality of the fibers produced.<sup>25-28</sup> In one such study, Wang and co-workers electrospun blends of PNIPAAm and polystyrene; the resultant nanofibers exhibited reversible superhydrophilicity and superhydrophobicity when the temperature was varied between 20 °C and 50 °C.<sup>29</sup> Lin *et al.* explored PNIPAAm / poly(2-acrylamido-2-methylpropanesulfonic acid) nanofibers, and found that drug release at temperatures below the LCST was faster than when experiments were performed above the LCST.<sup>30</sup> In other work, Song produced PNIPAAm / poly(ethylene oxide) (PEO) composite nanofibers.<sup>31</sup> The fibers were loaded with vitamin B12 as a model hydrophilic drug, and the release profile could be modulated by varying the PEO/PNIPAAm ratio, the release temperature, and the drug loading. In

this work, we aimed to expand on these earlier investigations to develop enhanced understanding of the properties of electrospun PNIPAAm blends with other polymers.

Ketoprofen (KET), a non-steroidal anti-inflammatory drug, has been widely used for the treatment of inflammation, pain and rheumatism but suffers from very poor water solubility (0.5 µg/ml).<sup>32</sup> It also has a short biological half-life (1.5 to 2 hours).<sup>33</sup> Commercially it is available as a number of formulations, including ketoconazole and ketolac. The dosing regimen is 50-100 mg twice a day.<sup>32</sup> Therefore, it is desirable to develop controlled release formulations of KET to increase patient convenience and reduce side effects.

In this study, KET was chosen as a model drug for the development of controlled release formulations. It was blended with PNIPAAm and ethylcellulose (EC, an inert, water-insoluble, non-toxic polymer widely used to prepare slow-release formulations) and electrospun into fibers.<sup>34,35</sup> By combining these three components, we aimed to produce thermoresponsive sustained release formulations of KET. These could be used to ensure that the drug concentration in the body remains within the therapeutic window for prolonged periods of time, minimizing over- or underdosing and maximizing therapeutic benefit and patient convenience.

## **2. Experimental**

### **2.1 Materials**

N-isopropylacrylamide (NIPAAm) was purchased from Japan TCI (Tokyo, Japan). Ethyl cellulose (EC, 6-9 m Pa·s) was obtained from the Aladdin Chemistry Co., Ltd. (Shanghai, China). Ketoprofen (KET) was purchased from the Beijing J&K Scientific Co., Ltd. (Beijing, China). L929 cells (a mouse fibroblast cell line) were obtained from the Institute of Biochemistry and Cell Biology (Chinese Academy of Sciences, Shanghai, China). DMEM medium, thiazolyl blue (MTT reagent), fetal bovine serum (FBS), phosphate-buffered saline (PBS), penicillin and streptomycin were purchased from the Nanjing keyGEN Biotechnology Co., Ltd. (Nanjing, China). Tween-80 and dimethyl sulfoxide (DMSO) were provided by the Sinopharm Chemical Reagent Co.,

Ltd. (Shanghai, China). Acetone was purchased from the Yonghua Chemical Technology Co., Ltd. (Suzhou, China), while azobisisobutyronitrile (AIBN) was provided by the Shisi Hewei Chemical Co., Ltd. (Shanghai, China). Anhydrous ether and anhydrous ethanol were obtained from the Changshu Hongsheng Fine Chemical Co., Ltd. (Suzhou, China). All chemicals were of analytical grade and used directly without further purification. Water was deionized prior to use.

## **2.2 Synthesis of PNIPAAm**

A solution of NIPAAm (5.00 g) and AIBN (25.00 mg) in 10 mL of anhydrous ethanol was degassed and heated to 70 °C under a positive pressure of N<sub>2</sub>. After 7 h, the resultant polymer was precipitated in anhydrous ether. The crude product was then reprecipitated from 50 mL of acetone into 200 mL of anhydrous ether three times, to yield 4.20 g (84%) of a pure product. Successful synthesis was verified by IR and NMR spectroscopies, and gel permeation chromatography (see Supporting Information).

## **2.3 Preparation of electrospinning solutions**

PNIPAAm and EC were dissolved in anhydrous ethanol under magnetic stirring for 12 h at room temperature, resulting in clear and homogenous solutions. The total concentration of polymer was 25 % (w/v). KET was added into certain solutions at a drug to polymer ratio of 1:4 (w/w). The viscosity of the electrospinning solutions was measured using a viscometer (CAP 2000+, Brookfield Co. Ltd., USA). Full details of the solutions prepared are listed in Table 1.

## **2.4 Electrospinning**

The electrospinning solution was placed into a 5 mL plastic syringe fitted with a stainless steel needle (internal diameter 0.5 mm), and the syringe was mounted on a syringe pump (KDS100, Cole-Parmer, Vernon Hills, IL, USA). During spinning, the flow rate of the solution was maintained at 0.5 mL / h. The needle was charged with a positive voltage of 13 kV, provided by a high voltage power supply (ZGF-2000,

Shanghai Sute Electrical Co., Ltd., Shanghai, China). The working distance between the needle tip and the grounded collector was fixed at 10 cm. The resultant fibers were collected on a flat plate coated with aluminum foil, and subsequently dried at 25 °C in a vacuum oven (DZF-6050, Shanghai Laboratory Instrument Work Co. Ltd., Shanghai, China) for 24 h to remove any residual solvent.

## 2.5 Characterization

The surface morphology of the fibers was analyzed with scanning electron microscopy (SEM; JSM-5600 LV microscope, JEOL, Tokyo, Japan). Samples were gold sputter-coated for 60 s under argon to render them electrically conductive prior to visualization. The average fiber diameter for each sample was calculated by measuring approximately 50 fibers in SEM images using the ImageJ software (National Institutes of Health, Bethesda, MD, USA). Selected nanofibers were also investigated using a transmission electron microscope (TEM, H-800 instrument, Hitachi, Tokyo, Japan). The accelerating voltage during TEM experiments was 200 kV.

X-ray diffraction (XRD) was undertaken on a D/Max-BR diffractometer (Rigaku, Tokyo, Japan) with Cu K $\alpha$  radiation (40 kV / 20 mA) over the 2 $\theta$  range 5 to 60°. Fourier transform infrared (FTIR) analysis was carried out on a Nicolet-Nexus 670 spectrometer (Nicolet Instrument Corporation, Madison, WI, USA) over the range 4000 – 500 cm<sup>-1</sup> and with a resolution of 2 cm<sup>-1</sup>. Samples were prepared using the KBr disk method (2 mg sample in 200 mg KBr).

The water contact angle (CA) was determined on a contact angle analyzer (DSA 30, Krüss GmbH, Hamburg, Germany) in air. A water droplet (*ca.* 2  $\mu$ L) was placed onto the surface of the fibers and the CA recorded. The measurement temperature was controlled using a heating platform (XMTD-204, JTHF Company, Jintan, China). Five measurements were recorded for each sample, and the results are reported as mean  $\pm$  S.D.

## 2.6 Molecular modelling

Molecular mechanics calculations were undertaken using HyperChem version 8.0.10. The structures of each of the compounds were first drawn using ChemBio Draw Ultra 14.0. A decameric EC or PNIPAAm species was constructed to represent the polymer. The individual structures were then imported into HyperChem, and models constructed as detailed in previous work. Combinations of the energy minimised polymer-KET structures were then merged to create drug-polymer complexes, and these were subjected to the same minimisation procedures to determine whether they were energetically stabilised in relation to the individual components. This procedure is similar to that previously reported by Dott *et al.*<sup>36</sup>

### **2.7 *In vitro* drug release**

For *in vitro* drug release studies, 80 mg of each sample was immersed in a plastic bottle filled with 20 mL of phosphate buffer solution (PBS, pH 7.4) containing 0.05 % v/v Tween-80 to enhance the solubility of KET. The bottle was incubated in a shaker bath at two different temperatures (25 or 37 °C) at a shaking rate of 90 rpm. At predetermined time points, 1.4 mL of the PBS solution was removed to quantify the drug concentration, and 1.4 mL of fresh buffer solution added to maintain the total solution volume. The concentration of KET was measured using a UV-vis spectrometer (UV-1800, SHJH Company, Shanghai, China) at a wavelength of 265 nm, following construction of an appropriate calibration curve. All the release studies were performed in triplicate, and the results are given as mean  $\pm$  S.D.

### **2.8 Cell viability experiments**

Nanofibers were collected directly onto coverslips by electrospinning. 36 coverslips were placed on the collector and electrospinning performed as detailed in Section 2.4, for 4h. The coated slides were placed in 24-well plates (1 slide per well), with untreated slides used as negative controls. The loaded plates were disinfected with ultraviolet irradiation for 24 h.

L929 fibroblasts cells were cultured in DMEM medium supplemented with penicillin (100 units / mL), streptomycin (100  $\mu$ g / mL), and 10 % (v/v)

heat-inactivated fetal bovine serum. Trypsinization was used to detach the cells from the culture flask, and 200  $\mu\text{L}$  of dissociated L929 cells were seeded into the sterilized 24-well plates at a density of  $4 \times 10^3$  cells per well. After 1, 3 or 5 days incubation (37  $^{\circ}\text{C}$ , 5 %  $\text{CO}_2$ ), the culture medium in each well was removed and replaced with 360  $\mu\text{L}$  of fresh DMEM and 40  $\mu\text{L}$  of MTT solution (5 mg / mL thiazolyl blue in PBS). Following incubation for 4 h (37  $^{\circ}\text{C}$ , 5 %  $\text{CO}_2$ ), the medium was removed and 400  $\mu\text{L}$  of DMSO added to each well, after which the plates were shaken for 20 min at 37  $^{\circ}\text{C}$ . The solution from each well was transferred into a 96-well plate, and then the absorbance measured at a wavelength of 570 nm using a microplate reader (Multiskan FC, Thermo Scientific Instrument Co. Ltd., Shanghai, China). Three independent MTT assays were carried out, with 6 replicates per assay.

### **3. Results and discussion**

#### **3.1 Morphology analysis**

Scanning electron microscopy (SEM) images of the fibers are shown in Fig. 1. The viscosities of the electrospinning solutions are listed in Table 1. F1, F2, F4, and F5 exhibit some flat ribbon-like fibers, with this being particularly evident for F1 and F4 where PNIPAAm is the sole polymer present and solution viscosity is low (less than 200 cP). Some beads are also observed on the surface of F2 and F5. These fibers are formed from EC solutions for which the viscosity is very high (more than 300 cP). Combining EC and PNIPAAm results in highly uniform fibers (F3), with no beads visible and no ribbon-like fibers. Similarly regular cylindrical fibers are observed when KET is introduced to the polymer blend (F6, F7, F8). Combining EC and PNIPAAm thus appears to aid the formation of smooth fibers. The addition of EC to the PNIPAAm solution results in higher viscosity which increases the electrospinnability and aids the formation of smooth fibers.<sup>37</sup> When the viscosity is too high (as is the case with the pure EC solutions), beaded fibers (F2, F5) form because the solution becomes difficult to force through the syringe needle, making the solution flow rate somewhat unstable.<sup>38, 39</sup> The ideal



viscosity for this system appears to lie between 200 cP and 300 cP.

Transmission electron microscopy (TEM) images of F3 and F6 are also given in Fig. 1. As would be expected for the products of a single-fluid electrospinning process, the fibers are monolithic in nature, with no evidence of any phase segregation. Both the SEM and TEM images indicate that drug particles do not separate from the drug loaded fibers during solvent evaporation.

The diameters of the fibers are given in Table 1. The diameters of the drug loaded nanofibers (F4, F5, F6) are larger than those which consist of polymer alone (F1, F2, F3). The F3, F6, F7 and F8 materials are more uniform in their diameters than the other systems. The fibers containing only EC as the filament forming polymer (F2, F5) are narrower than those made of PNIPAAm (F1, F4), with the blend fibers (F3, F6, F7, F8) being intermediate in size.

### 3.2 Physical form analysis and component compatibility

X-ray diffraction patterns are given in Fig. 2A. Pure KET shows well-defined Bragg reflections at  $6.4^\circ$ ,  $13.2^\circ$ ,  $14.5^\circ$ ,  $18.4^\circ$ ,  $20.1^\circ$ ,  $21.8^\circ$ ,  $22.9^\circ$ ,  $23.9^\circ$ ,  $26.1^\circ$  and  $29.6^\circ$   $2\theta$ , demonstrating its crystalline nature. PNIPAAm (F1) displays two broad diffuse features centered at around  $8^\circ$  and  $21^\circ$ , consistent with its well-known amorphous physical form.<sup>31</sup> EC (F2) also displays two broad diffuse peaks, again indicating an amorphous state.<sup>40</sup> The pattern of F3 demonstrates that, as would be expected, the blend fibers are also amorphous. The KET-loaded materials F4, F5 and F6 additionally show no Bragg reflections, which demonstrates that the drug has been converted to the amorphous physical form by electrospinning.

The FTIR spectra of KET and the fibers are presented in Fig. 2B. F1 (PNIPAAm fibers) shows a broad band between *ca.*  $3700$  and  $3100\text{ cm}^{-1}$ , which comprises a superposition of H-bonded N-H stretches ( $3296\text{ cm}^{-1}$ ) as well as Amide I and II combinations and overtone bands.<sup>41</sup> It also has a series of absorptions at  $2750 - 3000\text{ cm}^{-1}$  arising from  $\text{CH}_3$ ,  $\text{CH}_2$  and  $\text{CH}$  stretches, and distinct peaks at  $1645\text{ cm}^{-1}$  ( $\text{C}=\text{O}$  stretching vibration) and  $1548\text{ cm}^{-1}$  ( $\text{C}-\text{N}$  stretching and N-H bending vibrations). Vibrations at lower wavenumbers correspond to  $\text{CH}_3$ ,  $\text{CH}_2$  and  $\text{CH}$  bends. F2 (EC

alone) shows characteristic peaks at  $3476\text{ cm}^{-1}$  (OH group vibrations),  $2750 - 3000\text{ cm}^{-1}$  ( $\text{CH}_3$ ,  $\text{CH}_2$  and  $\text{CH}$  stretches) and  $1109\text{ cm}^{-1}$  C-O-C stretching).<sup>42</sup> Very similar absorptions are present in F3, the blend fibers. However, there are some small shifts in peak positions (*e.g.* from  $3296\text{ cm}^{-1}$  in F1 to  $3307\text{ cm}^{-1}$  in F3, and from  $1645\text{ cm}^{-1}$  in F1 to  $1654\text{ cm}^{-1}$  in F3), which indicate the presence of intermolecular bonding interactions between the two polymer components.

Considering the drug-loaded fibers, the major peaks from the polymers are again visible, also with small red shifts from *e.g.*  $3296\text{ cm}^{-1}$  in F1 to  $3295\text{ cm}^{-1}$  in F4, from  $1548\text{ cm}^{-1}$  in F1 to  $1545\text{ cm}^{-1}$  in F4; or from  $1109\text{ cm}^{-1}$  in F2 to  $1107\text{ cm}^{-1}$  in F5. The OH absorbances at  $3466\text{ cm}^{-1}$  in F5 and F6 are also red shifted compared with pure EC (F2), where this stretch is located at  $3476\text{ cm}^{-1}$ .

The FTIR spectrum for pure ketoprofen shows two distinct peaks: one at  $1696\text{ cm}^{-1}$  representing the stretching vibration of the carbonyl group in the KET dimer, and another at  $1655\text{ cm}^{-1}$  from stretching of the ketone group. The peak at  $1696\text{ cm}^{-1}$  is observed because in its crystalline form KET molecules are bound together in dimers through intermolecular hydrogen bonds. The peak at  $1655\text{ cm}^{-1}$  is present in the spectra of F4, F5 and F6, which indicates the presence of KET in these samples. It is however shifted somewhat: in F4, this peak is merged with the PNIPAAm C=O stretch into a single peak at  $1645\text{ cm}^{-1}$ , and in F5 is moved to  $1658\text{ cm}^{-1}$ . The peak at  $1696\text{ cm}^{-1}$  cannot be seen in the spectra of F4, F5 and F6, indicating the absence of any KET dimers in the fibers. This is consistent with the result of X-ray diffraction analysis, which showed the absence of any crystalline (dimeric) KET.

### 3.3 Molecular modelling

Since KET has C=O groups, EC has -OH groups, and PNIPAAm has NH groups, it is to be expected that there will be H-bonding interactions between KET and EC or KET and PNIPAAm.<sup>37</sup> The shifts in peak positions identified in the IR spectra indicated that such interactions do indeed occur in the fibers; to confirm this, we constructed some simple molecular models of EC, PNIPAAm and KET using the HyperChem software. The structures of an EC or PNIPAAm decamer and KET were first

individually optimized, and subsequently appropriate combinations of the energetically minimized structures were merged to create drug-polymer complexes. The geometric preferences for the energetically minimized EC-PNIPAAm and KET-polymer complexes are depicted in Fig. 3. The energetic contributions to the overall steric energies are listed in Table 2.

It is clear from the data in Table 2 that, as was indicated from the IR spectra, there are a number of intermolecular interactions (both van der Waals and H-bonding) between the drug and polymers, as well as between PNIPAAm and EC. Stabilisation of the complexes is indicated by a negative difference between the total steric energy of the complex and the sum of the energies of the individual molecules ( $\Delta E = E_{\text{complex}} - \Sigma E_{\text{components}}$ ). The combined steric energy of PNIPAAm and KET is 15.974 kcal / mol, whereas that of the complex is 0.315 kcal mol<sup>-1</sup>. This gives a  $\Delta E$  of - 15.659 kcal / mol. For EC-KET  $\Delta E = -17.021$  kcal / mol, and for PNIPAAm-EC  $\Delta E = -9.557$  kcal / mol. Thus, in all cases there are favorable stabilizing interactions between the components of the system; these comprise both van der Waals and H-bonding interactions.

### 3.4 Thermoresponsive behavior

The wettability of the nanofibers was studied as a function of temperature, and the results are depicted in Fig. 4A. The water contact angles of the drug-free and analogous drug-loaded nanofibers are basically identical (F1 *cf.* F4; F2 *cf.* F5; F3 *cf.* F6). The addition of KET thus has little influence on the contact angles. The pure EC fibers are hydrophobic regardless of the temperature, with only a very small increase in contact angle seen across the temperature range studied. In contrast, as the temperature is raised from 25 °C to 45 °C, the surfaces of the PNIPAAm-containing fibers change abruptly from being hydrophilic to hydrophobic. This occurs as the temperature increases through the LCST between 31 °C and 33 °C, and results in a dramatic increase in the contact angle.

Fig. 4B shows the proposed mechanism underlying the thermoresponsive properties of the PNIPAAm/EC composite nanofibers. When the temperature is below

the LCST (32 °C), the hydrophilic C=O and N-H groups in the PNIPAAm chains interact easily with water molecules to form intermolecular hydrogen bonds.<sup>43</sup> Although there are hydrophobic EC molecules also present in the blend fibers, the water droplets can presumably minimize their contact with these and maximize their interactions with PNIPAAm units. Consequently, the blend fibers exhibit hydrophilic properties below the PNIPAAm LCST. When the temperature is above the LCST, the formation of intramolecular hydrogen bonds between the C=O and N-H groups in PNIPAAm lead to a collapsed globular conformation of the chains, which makes it very hard for their C=O and N-H groups to interact with water molecules.<sup>29</sup> Therefore, the blend fibers are hydrophobic above the LCST.

### 3.5 Drug release

*In vitro* KET release profiles of KET from the drug loaded nanofibers are given in Fig. 5. Considering first the data in Fig. 5A (1:2 PNIPAAm/EC systems), at 25 °C, the amount of drug release from F4 (PNIPAAm) is highest, followed by F7 (PNIPAAm/EC 1:2 w/w) and F5 (EC). The different drug release profiles may be explained by the fibers' different surface wettability. Drug release from a hydrophilic carrier tends to be faster than that from a hydrophobic material.<sup>30</sup> When the temperature is 25 °C, the PNIPAAm-containing fibers exhibit hydrophilic properties, while the EC materials are hydrophobic. The fibers comprising only PNIPAAm as the filament-forming polymer are more hydrophilic than the blend fibers, explaining why the latter lies intermediate between the two extremes. At 37 °C, there is a burst release of roughly 40% of the loaded drug in the first 5 h of the dissolution experiment. Very little further release is seen from F4, while F5 and F6 show slow, sustained, release over *ca.* 55 h. F6 releases most drug under these conditions, followed by F5 and F4.

The drug release profile from the EC fibers (F5) is very similar at both temperatures investigated. This is because EC is not thermoresponsive, but can be used as a sustained-release drug delivery system. In contrast, the maximum drug release from the PNIPAAm-containing fibers is much greater at 25 °C than at 37 °C, as a result of the temperature sensitive properties of PNIPAAm. However, at both

temperatures the F4 fibers show a very significant burst release at the start of the experiment. These effects are somewhat reduced for the PNIPAAm/EC F6 samples, indicating that the blend nanofibers combine the advantages of the two polymers, possessing both thermosensitive and sustained release properties. These results thus demonstrate the concept of using PNIPAAm/EC blend fibers for temperature-triggered sustained release.

The influence of the PNIPAAm/EC weight ratios was also explored, and a comparison of F6, F7 and F8 are presented in Fig. 5B. At 25 °C, the amount of drug released from F7 (PNIPAAm/EC 1:1) is highest, followed by F6 (1:2) and F8 (1:4). At 37 °C, the opposite trend is seen. These observations indicate that an increased content of EC decreases the drug release rate at 25°C but increases it at 37°C. This is to be expected, since PNIPAAm becomes hydrophobic at  $T > 32$  °C but is hydrophilic below this temperature. Thus, at 25 °C the hydrophilic nature of the PNIPAAm increases the rate of release, and F7 (which contains most PNIPAAm) releases its KET load most rapidly. At 37 °C, the hydrophobic nature of the PNIPAAm delays release; thus, the more PNIPAAm present the slower the drug release rate, and F7 releases most slowly under these conditions. The drug release profiles from F8 (PNIPAAm/EC 1:4) are similar at both temperatures investigated; the low PNIPAAm content in this system is presumably insufficient to provide it with significant thermoresponsive properties.

### **3.6 Cell viability**

The results of MTT cell viability measurements performed on the fibers are given in Fig. 6. As expected, the number of cells present increased from day 1 to day 5 in all cases. The cell viability of analogous drug-free fibers and drug-loaded fibers are almost identical. Compared to the negative control (blank coverslips), there is a noticeable reduction in cell growth with F1 and F4. There is also possibly a much smaller decrease with F3 and F6, and a small increase in cell number with F2 and F5. From these observations, it can be inferred that the surfaces of EC nanofibers are

more suitable for cell growth than those of PNIPAAm. As a result, the cell number observed with F3 (F6) is intermediate between F1 (F4) and F2 (F5). Overall however, the viability of cells grown on the PNIPAAm/EC fibers is high, which is very promising for potential biomedical applications.

#### **4. Conclusions**

Nanoscale fibers made of poly(N-isopropylacrylamide) (PNIPAAm), ethyl cellulose (EC) and blends of the two were prepared by electrospinning. Ketoprofen (KET) was selected as a model drug, and analogous drug-loaded fibers also generated. The blend fibers have more regular morphologies than the single-polymer materials. X-ray diffraction data demonstrate that KET exists in the amorphous physical form in the drug-loaded fibers. There are significant intermolecular interactions between KET and the polymers, as evidenced by IR spectroscopy and molecular modelling. The water contact angle of the PNIPAAm and blend nanofibers changes abruptly upon heating, increasing from  $45 \pm 2.5^\circ$  to  $124 \pm 4^\circ$  for the latter when the temperature is increased through the lower critical solution temperature of  $32^\circ\text{C}$ . The fibers thus undergo a rapid hydrophilic/hydrophobic transition at this point. With a 1:2 weight ratio of PNIPAAm/EC in the fibers, KET release at  $25^\circ\text{C}$  is much faster than at  $37^\circ\text{C}$  as a result of this dramatic change in properties. The same results are observed with a 1:1 ratio, but the release rate from the fibers is rather low at  $37^\circ\text{C}$ . When the PNIPAAm/EC ratio is raised to 1:4 the materials appear to lose most of their thermoresponsive properties. The blend fibers also proved to be non-toxic and suitable for cell growth. This study thus demonstrates that electrospun blend PNIPAAm/EC fibers can be used as thermoresponsive carriers for the sustained release of poorly water soluble drugs, as well as in tissue engineering.

#### **5. Acknowledgements**

This work was financially supported by the UK-China Joint Laboratory for Therapeutic Textiles (based at Donghua University).

## **6. References**

- 1.** He J-H 2007. Electrospinning: The big world of small fibers. *Polymer International* 56:1321-1322.
- 2.** Ding B, Kim HY, Lee SC, Shao CL, Lee DR, Park SJ, Kwag GB, Choi KJ 2002. Preparation and characterization of a nanoscale poly (vinyl alcohol) fiber aggregate produced by an electrospinning method. *Journal of Polymer Science Part B: Polymer Physics* 40:1261-1268.
- 3.** Brettmann B, Bell E, Myerson A, Trout B 2012. Solid-state NMR characterization of high-loading solid solutions of API and excipients formed by electrospinning. *Journal of Pharmaceutical Sciences* 101:1538-1545.
- 4.** Feng L, Li S, Li H, Zhai J, Song Y, Jiang L, Zhu D 2002. Super-hydrophobic surface of aligned polyacrylonitrile nanofibers. *Angewandte Chemie* 114:1269-1271.
- 5.** Martin CR 1996. Membrane-based synthesis of nanomaterials. *Chemistry of Materials* 8:1739-1746.
- 6.** Ma PX, Zhang R 1999. Synthetic nano-scale fibrous extracellular matrix. *Journal of Biomedical Materials Research* 46:60-72.
- 7.** Whitesides GM, Grzybowski B 2002. Self-assembly at all scales. *Science* 295:2418-2421.
- 8.** Tsaroom A, Matyjaszewski K, Silverstein MS 2011. Spontaneous core-sheath formation in electrospun nanofibers. *Polymer* 52:2869-2876.
- 9.** Sahoo S, Ang LT, Goh JCH, Toh SL 2010. Growth factor delivery through

electrospun nanofibers in scaffolds for tissue engineering applications. *Journal of Biomedical Materials Research Part A* 93:1539-1550.

**10.** Balogh A, Farkas B, Faragó K, Farkas A, Wagner I, Van Assche I, Verreck G, Nagy ZK, Marosi G 2015. Melt-Blown and Electrospun Drug-Loaded Polymer Fiber Mats for Dissolution Enhancement: A Comparative Study. *Journal of Pharmaceutical Sciences* 104:1767-1776.

**11.** Nagy ZK, Balogh A, Drávavölgyi G, Ferguson J, Pataki H, Vajna B, Marosi G 2013. Solvent-free melt electrospinning for preparation of fast dissolving drug delivery system and comparison with solvent-based electrospun and melt extruded systems. *Journal of Pharmaceutical Sciences* 102:508-517.

**12.** Ding B, Wang M, Wang X, Yu J, Sun G 2010. Electrospun nanomaterials for ultrasensitive sensors. *Materials Today* 13:16-27.

**13.** Pham QP, Sharma U, Mikos AG 2006. Electrospinning of polymeric nanofibers for tissue engineering applications: a review. *Tissue Engineering* 12:1197-1211.

**14.** de las Heras Alarcón C, Pennadam S, Alexander C 2005. Stimuli responsive polymers for biomedical applications. *Chemical Society Reviews* 34:276-285.

**15.** Nath N, Chilkoti A 2002. Creating “smart” surfaces using stimuli responsive polymers. *Advanced Materials* 14:1243-1247.

**16.** Schmaljohann D 2006. Thermo-and pH-responsive polymers in drug delivery. *Advanced Drug Delivery Reviews* 58:1655-1670.

**17.** Plunkett KN, Zhu X, Moore JS, Leckband DE 2006. PNIPAM chain collapse depends on the molecular weight and grafting density. *Langmuir* 22:4259-4266.



- 18.** Mayo-Pedrosa M, Alvarez-Lorenzo C, Lacík I, Martinez-Pacheco R, Concheiro A 2007. Sustained release pellets based on poly (N-isopropyl acrylamide): Matrix and in situ photopolymerization-coated systems. *Journal of Pharmaceutical Sciences* 96:93-105.
- 19.** Yim H, Kent M, Mendez S, Balamurugan S, Balamurugan S, Lopez G, Satija S 2004. Temperature-dependent conformational change of PNIPAM grafted chains at high surface density in water. *Macromolecules* 37:1994-1997.
- 20.** Okuzaki H, Kobayashi K, Yan H 2009. Non-woven fabric of poly (N-isopropylacrylamide) nanofibers fabricated by electrospinning. *Synthetic Metals* 159:2273-2276.
- 21.** Wu XS, Hoffman AS, Yager P 1992. Synthesis and characterization of thermally reversible macroporous poly (N-isopropylacrylamide) hydrogels. *Journal of Polymer Science Part A: Polymer Chemistry* 30:2121-2129.
- 22.** Schild HG 1992. Poly (N-isopropylacrylamide): experiment, theory and application. *Progress in Polymer Science* 17:163-249.
- 23.** Huang SR, Lin KF, Lee CF, Chiu WY 2014. Synthesis and properties of thermoresponsive magnetic polymer composites and their electrospun nanofibers. *Journal of Polymer Science Part A: Polymer Chemistry* 52:848-856.
- 24.** Rockwood DN, Chase DB, Akins RE, Rabolt JF 2008. Characterization of electrospun poly (N-isopropyl acrylamide) fibers. *Polymer* 49:4025-4032.
- 25.** Gu SY, Wang ZM, Li JB, Ren J 2010. Switchable Wettability of Thermo-Responsive Biocompatible Nanofibrous Films Created by Electrospinning.

Macromolecular Materials and Engineering 295:32-36.

- 26.** Chen M, Dong M, Havelund R, Regina VR, Meyer RL, Besenbacher F, Kingshott P 2010. Thermo-responsive core– sheath electrospun nanofibers from poly (N-isopropylacrylamide)/polycaprolactone blends. *Chemistry of Materials* 22:4214-4221.
- 27.** Wang J, Sutti A, Wang X, Lin T 2011. Fast responsive and morphologically robust thermo-responsive hydrogel nanofibres from poly (N-isopropylacrylamide) and POSS crosslinker. *Soft Matter* 7:4364-4369.
- 28.** Tzeng P, Kuo CC, Lin ST, Chiu YC, Chen WC 2010. New Thermoresponsive Luminescent Electrospun Nanofibers Prepared from Poly [2, 7-(9, 9-dihexylfluorene)]-block-poly (N-isopropylacrylamide)/PMMA Blends. *Macromolecular Chemistry and Physics* 211(13):1408-1416.
- 29.** Wang N, Zhao Y, Jiang L 2008. Low-Cost, Thermoresponsive Wettability of Surfaces: Poly (N- isopropylacrylamide)/Polystyrene Composite Films Prepared by Electrospinning. *Macromolecular Rapid Communications* 29:485-489.
- 30.** Lin X, Tang D, Cui W, Cheng Y 2012. Controllable drug release of electrospun thermoresponsive poly (N-isopropylacrylamide)/poly (2-acrylamido-2-methylpropanesulfonic acid) nanofibers. *Journal of Biomedical Materials Research Part A* 100:1839-1845.
- 31.** Song F, Wang X-L, Wang Y-Z 2011. Poly (N-isopropylacrylamide)/poly (ethylene oxide) blend nanofibrous scaffolds: Thermo-responsive carrier for controlled drug release. *Colloids and Surfaces B: Biointerfaces* 88:749-754.

- 32.** Gauri N, Aditi L, Shikha A, Dubey P 2011. Solubility enhancement of a poorly aqueous soluble drug ketoprofen using solid dispersion technique. *Der Pharmacia Sinica* 2:67-73.
- 33.** Kulkarni P, Dixit M, Kumar YS, Kini AG, Johri A 2010. Preparation and evaluation of Ketoprofen beads by melt solidification technique. *Der Pharmacia Sinica* 1:31-43.
- 34.** Crowley MM, Schroeder B, Fredersdorf A, Obara S, Talarico M, Kucera S, McGinity JW 2004. Physicochemical properties and mechanism of drug release from ethyl cellulose matrix tablets prepared by direct compression and hot-melt extrusion. *International Journal of Pharmaceutics* 269:509-522.
- 35.** Huang LY, Branford-White C, Shen XX, Yu DG, Zhu LM 2012. Time-engineered biphasic drug release by electrospun nanofiber meshes. *International Journal of Pharmaceutics* 436:88-96.
- 36.** Dott C, Tyagi C, Tomar LK, Choonara YE, Kumar P, du Toit LC, Pillay V 2013. A mucoadhesive electrospun nanofibrous matrix for rapid oramucosal drug delivery. *Journal of Nanomaterials* 924947.
- 37.** Sheng X, Fan L, He C 2013. Vitamin E-loaded silk fibroin nanofibrous mats fabricated by green process for skin care application. *International Journal of Biological Macromolecules* 56: 49-56.
- 38.** Deitzel J M, Kleinmeyer J, Harris D E A 2001. The effect of processing variables on the morphology of electrospun nanofibers and textiles. *Polymer* 42: 261-272.
- 39.** Pham Q P, Sharma U, Mikos A G 2006. Electrospinning of polymeric nanofibers

for tissue engineering applications: a review. *Tissue Engineering* 12: 1197-1211.

**40.** Huang LY, Yu DG, Branford-White C, Zhu LM 2012. Sustained release of ethyl cellulose micro-particulate drug delivery systems prepared using electrospraying. *Journal of Materials Science* 47:1372-1377.

**41.** Lizundia E, Meaurio E, Laza J, Vilas J, Isidro LL 2015. Study of the chain microstructure effects on the resulting thermal properties of poly (L-lactide)/poly (N-isopropylacrylamide) biomedical materials. *Materials Science and Engineering: C* 50:97-106.

**42.** Kang H, Liu W, He B, Shen D, Ma L, Huang Y 2006. Synthesis of amphiphilic ethyl cellulose grafting poly (acrylic acid) copolymers and their self-assembly morphologies in water. *Polymer* 47:7927-7934.

**43.** Lin X, Tang D, Gu S, Du H, Jiang E 2013. Electrospun poly (N-isopropylacrylamide) /poly (caprolactone)-based polyurethane nanofibers as drug carriers and temperature-controlled release. *New Journal of Chemistry* 37:2433-2439.

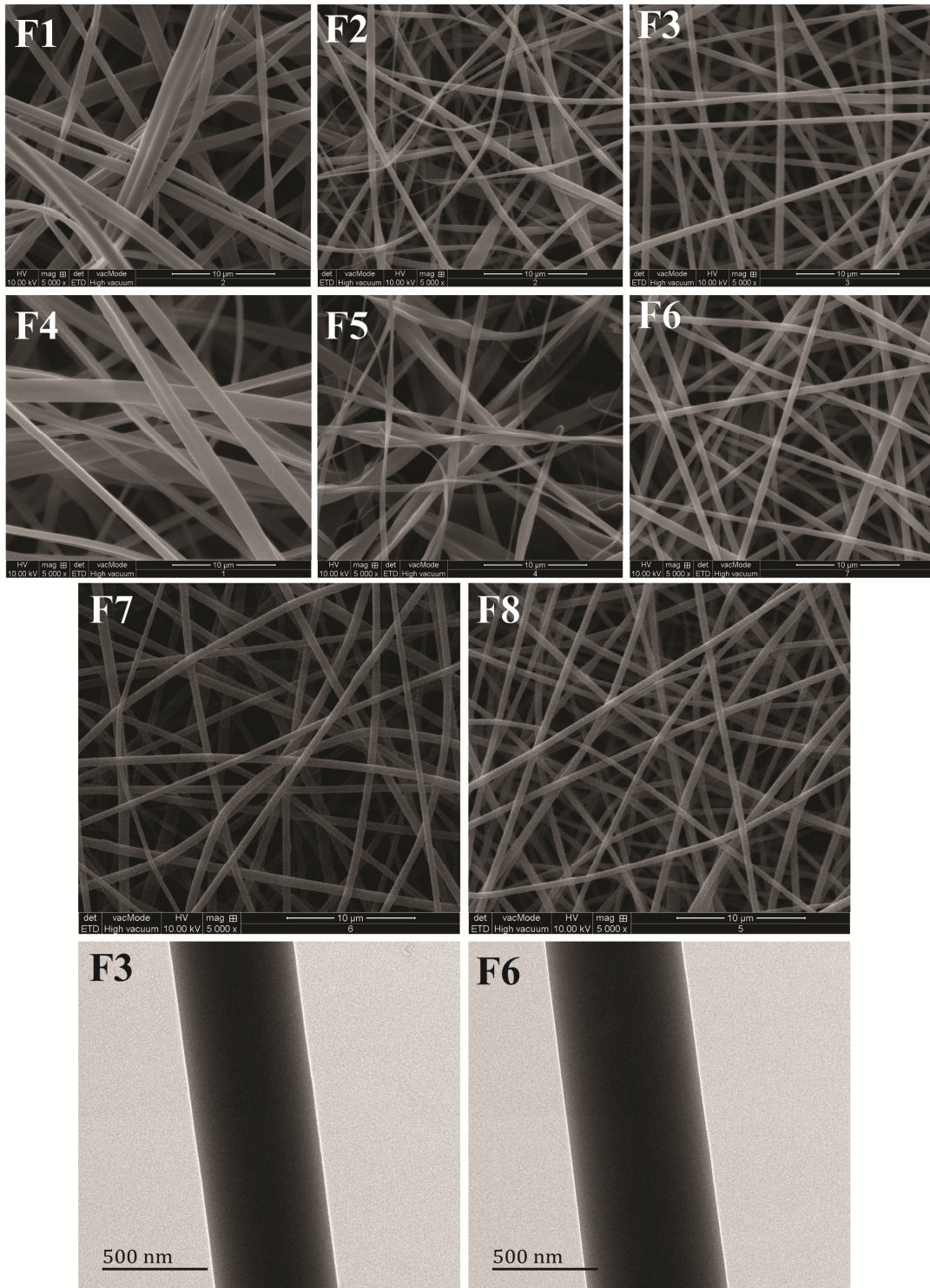


Fig. 1. SEM images of the fibers produced in this work, together with TEM images of F3 and F6. The scale bar at the bottom of all the SEM images corresponds to 10 μm.

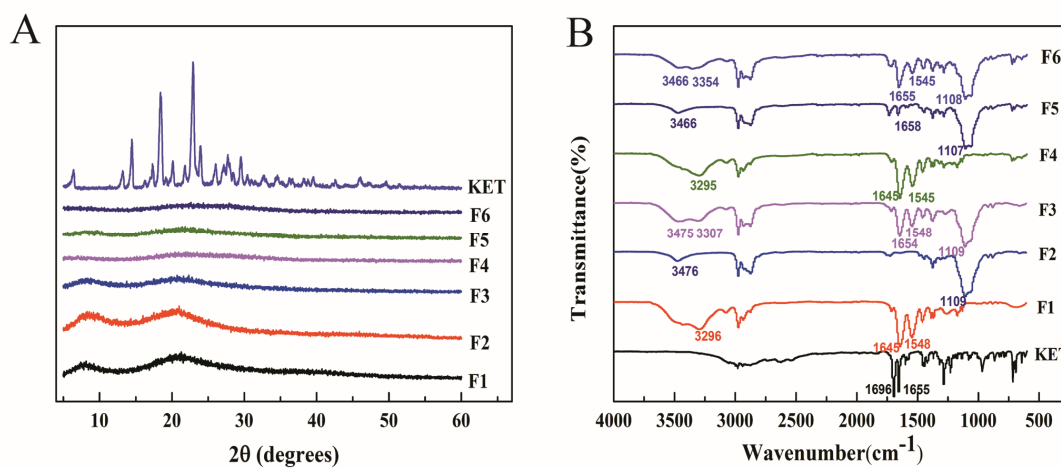


Fig. 2. A) XRD patterns and B) FTIR spectra of KET and selected fibers.

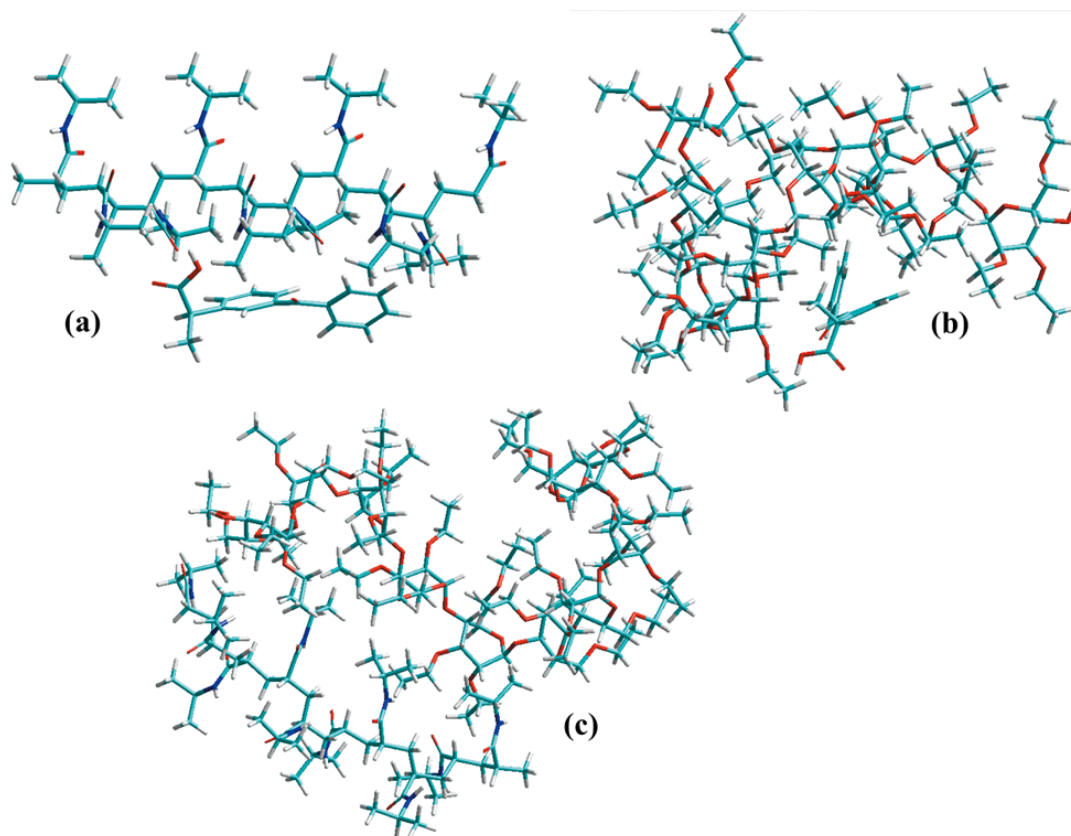


Fig. 3. The optimized geometric arrangements of A) PNIPAAm-KET, B) EC-KET, and C) PNIPAAm-EC. In A) and B), the polymer is at the top of the image and the drug molecule at the bottom; in C), EC is at the top and PNIPAAm at the bottom.

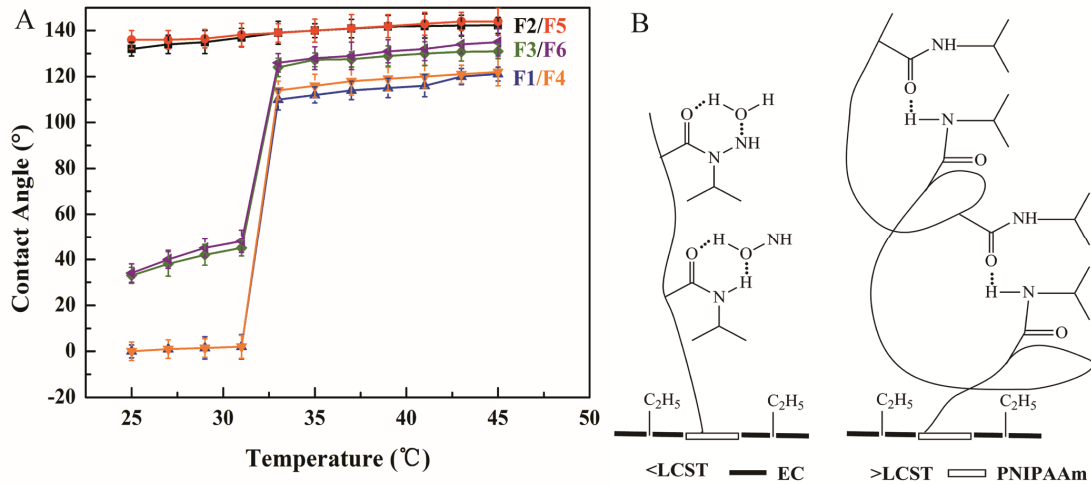


Fig. 4. A) The temperature dependence of the fibers' water contact angles and B) the proposed mechanism underlying the thermoresponsive properties of the PNIPAAm-containing fibers.

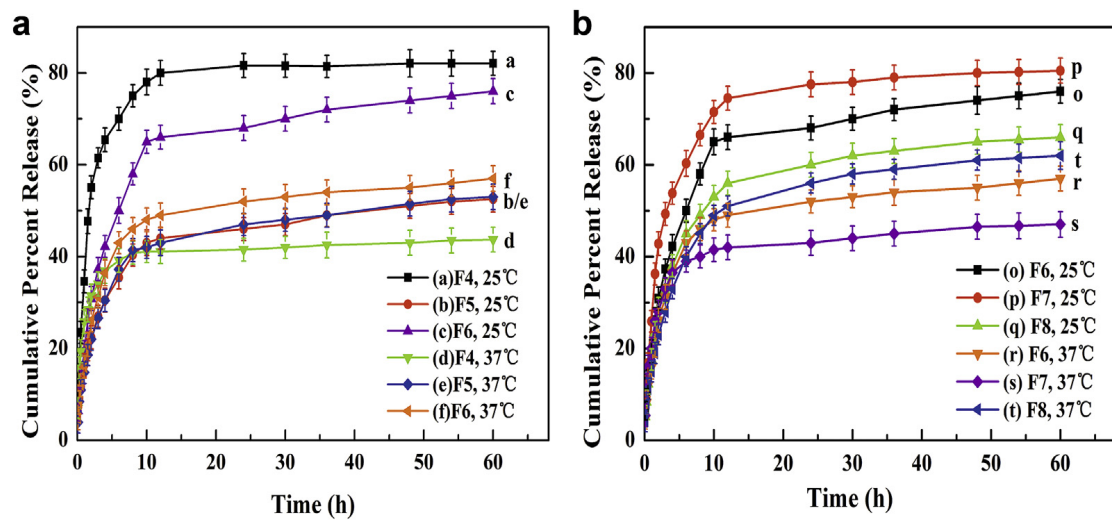


Fig. 5. *In vitro* KET release profiles from the electrospun fibers. The drug-loaded PNIPAAm (F4), EC (F5), and 1:2 blend (F6) materials are shown in A), while B) depicts the effect of changing the PNIPAAm: EC ratio from 1:2 (F6) to 1:1 (F7) and 1:4 (F8).

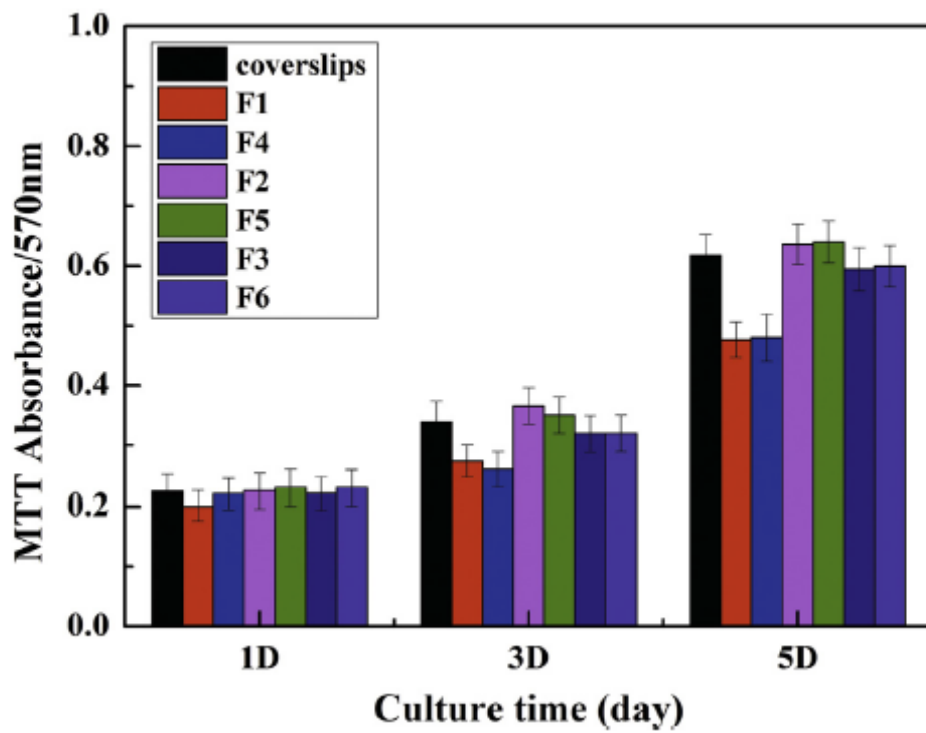


Fig. 6. The viability of L929 cells grown on blank coverslips and those coated with the fibers.



Table 1. Details of the spinning solutions used in this study.

ID	Solution content	PNIPAAm to EC ratio (w/w)	Total polymer conc. (% w/v)	Drug conc. (% w/v)	Mean diameter $\pm$ SD (nm)	Viscosity (cP)
F1	PNIPAAm	1:0	25	----	638 $\pm$ 157	68.4 $\pm$ 11.5
F2	EC	0:1	25	----	343 $\pm$ 110	309.2 $\pm$ 10.6
F3	PNIPAAm/EC	1:2	25	----	400 $\pm$ 56	235.6 $\pm$ 12.2
F4	PNIPAAm/KET	1:0	25	6.25	679 $\pm$ 191	92.3 $\pm$ 11.9
F5	EC/KET	0:1	25	6.25	415 $\pm$ 142	317.2 $\pm$ 11.2
F6	PNIPAAm/EC/KET	1:2	25	6.25	513 $\pm$ 72	242.4 $\pm$ 13.4
F7	PNIPAAm/EC/KET	1:1	25	6.25	532 $\pm$ 78	208.1 $\pm$ 13.7
F8	PNIPAAm/EC/KET	1:4	25	6.25	392 $\pm$ 63	286.5 $\pm$ 14.4

Table 2. Energetic values for the optimized KET, polymer, and KET-polymer complexes. The electrostatic contribution was found to be zero in all cases.

Species	Minimized energy combinations (kcal / mol)					
	Bond stretching	Bond angle	Torsional	Vander Waals	Hydrogen bonding	Total
KET	0.692	1.132	5.485	6.808	0.000	14.116
PNIPAAm	1.750	6.116	1.346	-7.336	-0.018	1.858
EC	6.752	48.182	101.722	-8.072	-0.539	148.045
PNIPAAm-KET	2.555	7.874	7.015	-16.826	-0.302	0.315
EC-KET	7.319	50.005	107.765	-19.409	-0.540	145.140
PNIPAAm-EC	8.463	55.851	108.998	-32.378	-0.587	140.346